A Wireless Accelerometer-Based Automatic Vehicle Classification Prototype System

Wenteng Ma, *Member, IEEE*, Daniel Xing, *Member, IEEE*, Adam McKee, Ravneet Bajwa, Christopher Flores, *Senior Member, IEEE*, Brian Fuller, and Pravin Varaiya, *Fellow, IEEE*

***Abstract*—Automatic vehicle classification (AVC) systems provide data about vehicle classes that are used for many purposes. This paper describes a prototype axle count and spacing AVC system using wireless accelerometers and magnetometers. The accelerometers detect vehicle axles, and the magnetometers report vehicle arrivals and departures and estimate speed. The prototype system is installed on Interstate 80 at Pinole, CA, USA, and tested under various traffic conditions. Video images and reports from a nearby commercial weigh-in-motion station provide ground truth to evaluate the performance of the system, including classification, axle spacing, and vehicle counts. The results show that the prototype AVC system is reliable in classifying vehicles even under congested traffic with accuracy of 99%.**

***Index Terms*—Accelerometer, automatic vehicle classification (AVC), axle count, axle spacing, magnetometer, wireless sensor.**

I. Introduction

VEHICLE classification data are collected for many purposes. For example, each state annually reports vehicle counts by class for the Highway Performance Monitoring System (HPMS). Automatic vehicle classification (AVC) is also the basis for intelligent transportation system applications and is important for traffic operation. For example, a freeway section with heavy truck traffic may require special rules to manage trucks. Pavement management processes pay special attention to trucks because they can make damage to the road surface. Toll collection systems may need AVC since tolls may vary by vehicle class.

Current AVC technologies have some deficiencies. Commercial systems using piezoelectric devices are expensive to install and maintain [1]. Nonintrusive technologies, such as video imaging and acoustic and infrared sensing, are sensitive to weather and lighting conditions [2]–[4]. Loop-based technologies do not perform well under congestion [5]. Methods based on vehicle length can only distinguish cars and trucks, and thus, are unsuited for applications that need more detailed classification, such as axle count and spacing [6]–[8].

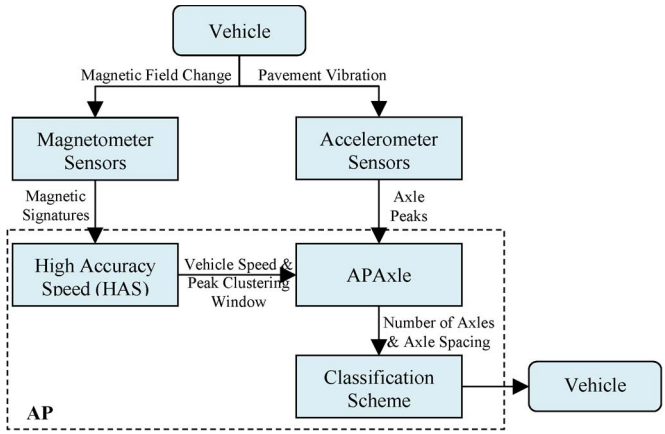

Fig. 1. AVC system architecture.

This paper describes a wireless sensor-based prototype AVC system that estimates the number of axles and axle spacing under both free flow and congested traffic. The system is based on the Sensys wireless vehicle detection system (VDS), which offers a reliable, accurate, and cost-effective sensing platform with the flexibility to address a wide range of traffic management applications [9], [10]. Each sensor can be installed in 10 min. The system is easy to maintain and can operate 24/7 under all weather conditions. VDS systems have been deployed around the world and have been operating continuously for many years, and 55000 new VDS systems were deployed in 2012 [11], [12].

This paper is organized as follows. A description of the prototype AVC system is given in Section II. A field study at Pinole, CA, USA, with ground-truth validation is described in Section III. Conclusions and further research are discussed in Section IV.

II. AVC System

A. System Architecture

The prototype AVC system includes two subsystems: The axle detection system uses accelerometer sensors to detect vehicle axles, and the speed measurement system uses magnetometers to estimate vehicle speed. As depicted in Fig. 1, accelerometers detect pavement vibration when a vehicle travels over their detection zones. The sensors locate the axle peaks

Manuscript received March 25, 2013; revised May 28, 2013 and July 2, 2013; accepted July 4, 2013. Date of publication August 15, 2013; date of current version January 31, 2014. This work was supported in part by the National Science Foundation through the Small Business Innovation Research Program under SBIR Phase I Award 0945919 and SBIR Phase II Award 1057566. The Associate Editor for this paper was M. Zhou.

W. Ma, D. Xing, A. McKee, R. Bajwa, C. Flores, and B. Fuller are with the Sensys Networks, Inc., Berkeley, CA 94710 USA (e-mail: wma@sensysnetworks.com; dxing@sensysnetworks.com; amckee@sensysnetworks.com; rbajwa@sensysnetworks.com; chrisf@sensysnetworks.com; brian@sensysnetworks.com).

P. Varaiya is with the Department of Electrical Engineering and Computer Sciences, University of California, Berkeley, CA 94720 USA (e-mail: varaiya@eecs.berkeley.edu).

Color versions of one or more of the figures in this paper are available online at http://ieeexplore.ieee.org.

Digital Object Identifier 10.1109/TITS.2013.2273488

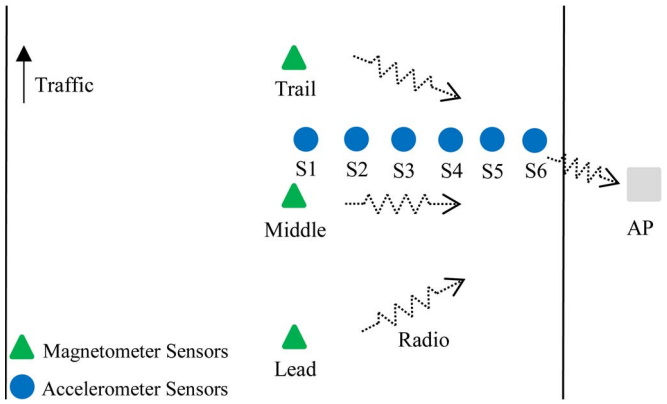

Fig. 2. AVC field installation prototype.

in the vibration data and send the peak location time to the access point (AP) installed by the roadside. Magnetometers perceive changes in the magnetic field caused by a vehicle and transmit the vehicle's magnetic signatures to the AP. The signatures are processed by the High Accuracy Speed (HAS) application running on the AP to calculate the speed and the peak clustering window to group axle peaks from the same vehicle. Another application, called APAxle, combines HAS data and accelerometer peak data to output the number of axles and axle spacing between each axle pair on a per vehicle basis. Using a predefined vehicle classification scheme, the class of the vehicle can be then determined and logged. The most common classification scheme, i.e., the FHWA 13-category Scheme F, is used in this paper [13]. The magnetometer sensors, accelerometer sensors, and the AP are all time synchronized to within 2 μs. Consequently, even if sensors report their measurements asynchronously, the AP can align magnetometer readings with the corresponding accelerometer readings.

B. Field Installation Prototype

The spatial configuration of the prototype AVC system is shown in Fig. 2. The blue circles represent accelerometer sensors, and the green triangles represent magnetometer sensors within one lane. Each sensor contains a transducer (accelerometer or magnetometer), a microprocessor, a radio, and a battery.

Typically, the accelerometer response dies down quickly when the tire of a vehicle is slightly offset from the accelerometer. To counter this effect and reduce the sensitivity requirement of the accelerometer, an array of accelerometer sensors (labeled S1, S2, . . ., S6) spaced closely together is necessary to guarantee that a tire rolls directly on top of at least one sensor. The installed accelerometer sensors need to cover at least half of the lane to detect the leftmost/rightmost tires. The lateral spacing between two adjacent sensors should be narrower than the smallest effective width of the tire of a target vehicle, which is usually 6–8 in.

Three magnetometer sensors (labeled Lead, Middle, and Trail) are needed for high speed/accuracy. They are usually placed close to the lane center. The vertical spacing is 4–6 ft so that individual vehicle will overlap all three sensors at one moment in time. This is important for distinguishing axle peaks from consecutive vehicles.

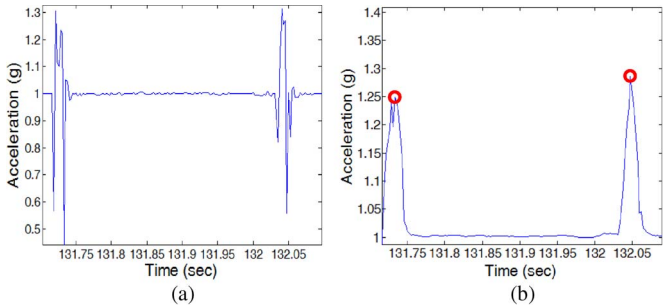

Fig. 3. Acceleration signal of a two-axle vehicle. (a) Raw signal. (b) Filtered signal.

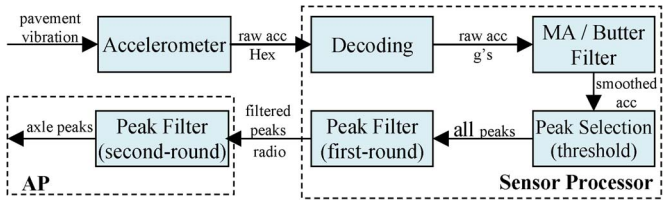

Fig. 4. Axle detection flowchart.

One AP (shown as the gray rectangle) is installed by the roadside. The sensors continuously transmit detection data via a low-power radio to the AP. Depending on the needs of the traffic application, the AP forwards the data to local traffic controllers, remote traffic management centers via wired or wireless connections, or both.

C. Axle Detection

When a vehicle's wheel moves across an accelerometer, the force causes the pavement to vibrate. The accelerometer measures these vibrations. The measurements are recorded and analyzed. Fig. 3 shows the acceleration signal of a two-axle vehicle that moves over an accelerometer. The x-axis is time in seconds, and the y-axis is acceleration in g (Note that, when no vehicle is present, the acceleration is 1 g). The two axles can be clearly identified from the raw signal shown in Fig. 3(a) without any filtering. However, to accurately calculate axle spacing and reliably identify tandem axles (whose spacing is usually 3–5 ft), an appropriate signal filter is needed to remove the noise from surrounding environment and smooth the signal. Fig. 3(b) shows the absolute value of the raw signal (relative to 1 g) after a moving average filter. The position of the circled peaks can be treated as the time when the axle tire is on top of the sensor. The time between peaks is inversely proportional to vehicle speed. If we know speed v, axle spacing d is

$$d = v \cdot t \tag{1}$$

where t is the time between the two peaks.

Fig. 4 depicts how the vibration data are processed in an accelerometer sensor. The pavement vibrations are captured by the accelerometer in hexadecimal values that are first decoded into acceleration g by a decoding function; then, the absolute value of the acceleration is smoothed by a signal filter (moving average/Butterworth). Acceleration values that exceed a preset threshold are selected and are considered peaks. Next, peak

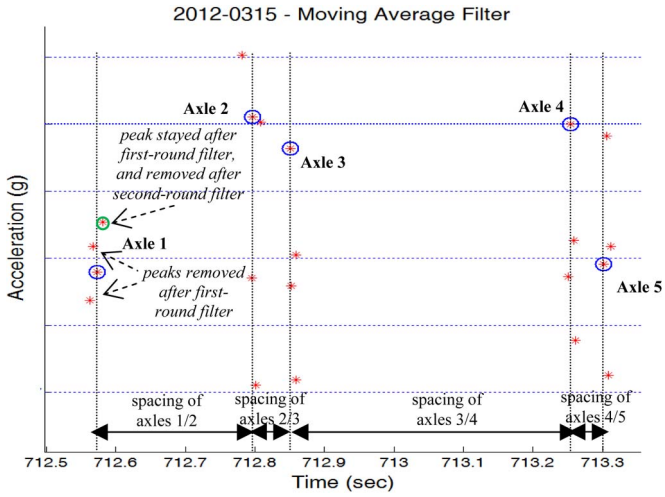

Fig. 5. Peak filter of a five-axle heavy truck sample.

filters are applied at both sensor level and AP level. At the sensor level, the first-round peak filter removes redundant peaks due to the noise of the highway environment; and at the AP level, the second-round peak filter removes redundant peaks generated across the accelerometer sensor array.

Fig. 5 shows the peak filter procedures for a five-axle truck. The red stars represent peaks from multiple sensors, and those with blue circles are the selected axle peaks after peak filters. The amplitude of the peak of each sensor is offset along the y-axis to facilitate visualization. As shown in Fig. 5, the truck is detected by six sensors labeled S1, S2, . . ., S6. The first axle is detected by S4 and S5 only, each outputs two peaks after the signal filter. The first-round peak filter is applied at the sensor level, and the sensor sends only the highest amplitude peak to the AP for the second-round peak filter. In this case, the one from S4 (green circle) is removed due to its lower amplitude, and the one from S5 is selected to represent the location of Axle 1. Similarly, the other four axles are all detected by multiple sensors, and their locations are represented only with the highest amplitude peaks (blue circles). The vehicle is therefore classified as a five-axle vehicle, and the spacing between the axles is estimated from the peak timestamps and the speed following (1).

D. Speed Measurement and Clustering

The magnetometer perceives a change in the magnetic field when a vehicle drives over it. The magnetic signatures of different vehicles are different, depending on the ferrous materials in the vehicle, as well as its size and orientation. The sensor also reports the time when a vehicle arrives at (an up event) and leaves (a down event) the detection zone. The up event and the down event are determined by comparing the vehicle's magnetic signature with prespecified threshold (see [14] for details). The data are delivered to HAS to calculate the speed and peak clustering window. A state machine determines whether the events originate from the same vehicle, particularly under congested traffic conditions.

HAS calculates vehicle speed in real time. Two types of speeds are reported, which differ in accuracy. Type 1 speed is based solely on up events. The magnetometer sensors, positioned along the direction of travel, report the timestamp when they first detect the front of the vehicle. The speed is calculated by dividing the spacing between the sensors by the time difference between up-event detection. This type of speed is subjected to sensor inaccuracies in sampling the vehicle's detection zone. Type 2 speed is calculated based on the magnetic signatures captured by the sensors. It is highly accurate (within speed error tolerance of ± 1 mi/h, [14]). Cross correlations of the signatures are used to determine the best time offset, which is used to correct the event-based Type 1 speeds. This measurement is important because it directly affects the accuracy of the axle spacing estimates. However, if valid comparisons between the signatures cannot be made, Type 1 speed serves as the backup for the speed calculation.

HAS also outputs a peak clustering window to decide which axles belong to the same vehicle. Usually, the left edge of the window is the up-event time of the Lead sensor, and the right edge is the down-event time of the Trail sensor (see Fig. 2). However, due to measurement noise, the up/down events might be missed or delayed. In this case, corresponding events from other magnetometer sensors in the set can be used as replacement. The missing events could also cause two successive vehicles to be incorrectly grouped as one vehicle if they are close together. On the other hand, sensors could fail to detect vehicle sections (e.g., a vehicle with a trailer) that do not have significant ferrous composition and report it as two vehicles. A best-effort approach based on typical vehicle specifications is applied to correct those errors. Axle spacing greater than the maximum specified wheelbase can dictate the splitting of a sample into two vehicles. For example, a four-axle vehicle would be considered two two-axle vehicles if its middle axle spacing is greater than a reasonable value (e.g., 60 ft). By contrast, if a vehicle is detected as a two-axle vehicle but its spacing is as small as tandem axle spacing, it could be considered a trailer and be grouped with its previous vehicle if they are close enough.

III. Case Study

A. Study Site

The prototype AVC system has been running continuously since it was installed on westbound Interstate 80 at Pinole, CA, USA, on March 12, 2012, as shown in Fig. 6. The top half of the figure is a bird's eye view of the study site. There are four lanes, and the system is installed in Lane 2 from the curb. An AP, a pan–tilt–zoom (PTZ) camera, and a hard drive are installed and can be remotely accessed via a cellular Internet connection. The camera is installed to take images to validate the system. Its rate is 3 fps, which is sufficient to capture vehicles at highway speeds. The lower half of the figure displays two sample images taken with the camera. The faint black dots within the white rectangle are the installed accelerometer and magnetometer sensors. The Coordinated Universal Time and local time are recorded at the top of each image. The images and sensor data are all stored on the hard drive.

The site is ideal for this paper since there is a Caltrans commercial weigh-in-motion (WIM) system 460 ft downstream

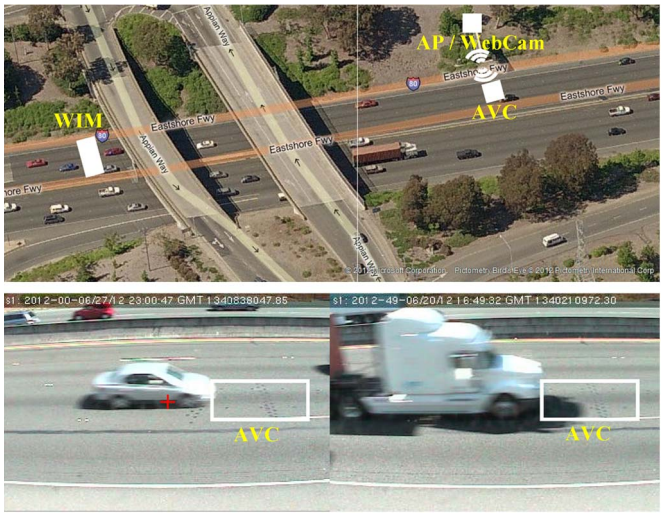

Fig. 6. Study site on west Interstate 80 at Pinole, CA, USA.

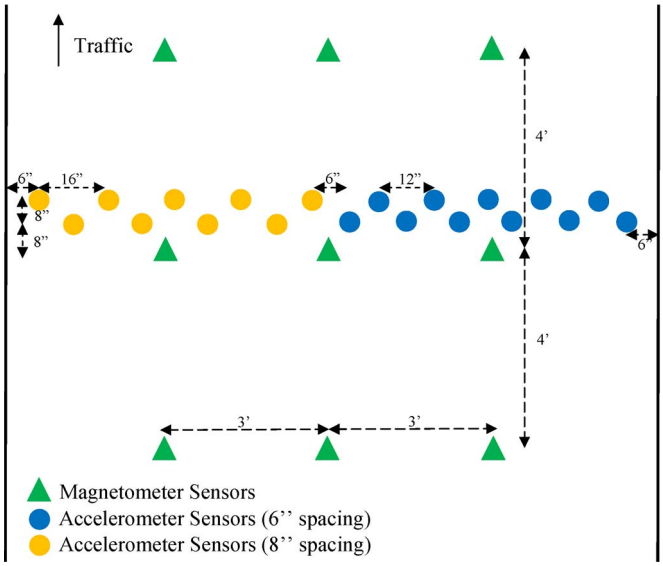

Fig. 7. AVC sensor installation layout at Pinole, CA, USA.

of the AVC system. The WIM system reports the axle counts, spacing, and weight of every truck. The reports can be used as an additional independent ground-truth source to validate the AVC system.

The sensor installation layout at Pinole, CA, USA, is depicted in Fig. 7. The blue and yellow circles are accelerometer sensors, and the green triangles are magnetometer sensors. The accelerometer sensors are staggered 8 in vertically to maintain the structural integrity of the road by not placing sensors too close to each other. To verify the best sensor installation spacing in a field highway environment, two sets of accelerometer sensors are installed. The nine sensors (yellow) on the left are 8 in apart, and the 11 sensors (blue) on the right are closer with spacing of 6 in. For the same purpose, three sets of magnetometer sensors are installed in the middle of the lane. The lateral distance between sets is 3 ft, and the vertical distance within each set is 4 ft.

B. Image Validation

1) Sensor Layout Selection: A 20-min data set was collected on March 15, 2012 from 10:25–10:45 A.M. Field images were recorded to evaluate the performance of the AVC system. Six scenarios with different accelerometer sensors and magnetometer sensor sets are compared:

- Scenario 1, where all 20 accelerometer sensors and all three magnetometer sensor sets are used;
- Scenario 2, where all the left nine 8-inch-spacing accelerometer sensors and the left and center magnetometer sensor sets are used;
- Scenario 3, where the right 11 6-in-spacing accelerometer sensors and the right and center magnetometer sensor sets are used;
- Scenario 4, where all 20 accelerometer sensors and the center magnetometer sensor set are used;
- Scenario 5, where the left nine 8-inch-spacing accelerometer sensors and all three magnetometer sensor sets are used;
- Scenario 6, where the right 11 6-inch-spacing accelerometer sensors and all three magnetometer sensor sets are used.

Fig. 8 shows a 10-s record of the vehicle classification plot of Scenario 6. The x-axis is time in seconds, and the y-axis is the peak acceleration from the right 11 accelerometer sensors. A pair of vertical lines illustrates the peak clustering window for a classified vehicle. The first dashed line shows the up-event time, and the second solid line shows the down-event time. The red stars are the peaks over the threshold, and the blue circled ones are the selected peaks after peak filters.

The performance of the scenarios is compared in Table I. In 20 min, 345 vehicles passed the detection zone. Among them, 299 were two-axle vehicles (i.e., passenger cars, light/medium trucks, and pickups), 3 were three-axle vehicles, and 43 were five-axle heavy trucks. Vehicle speeds varied from 32 to 80 mi/h. As expected, Scenario 1 gets the best performance and successfully classified all 345 vehicles. Scenarios 3 and 6 are also very good and only failed in 4 and 1 vehicles, respectively. On the other hand, Scenarios 2 and 5 missed more than 20 vehicles because the sensor spacing of the left set is wider than the effective tire width of some vehicles. Scenario 4 is considered the worst because it failed in five heavy trucks, which are usually more important in vehicle classification. As shown, heavy trucks are all correctly classified if all the three sets of the magnetometers are used, and with fewer sets, more trucks fail classification. The reason is that the up/down events could be delayed or missed when a heavy truck travels over the detection zone and degrades the radio channel, causing the loss of a data packet. In this case, multiple magnetometer sensor sets can recover the missed events and significantly improve the performance of the HAS system. It should be noted that vehicles during a lane-changing movement at the detection zone (not very common) are not included because only parts of the vehicle can be detected by the sensors. Based on the results in Table I, Scenario 6 is recommended in this paper, considering both performance and cost.

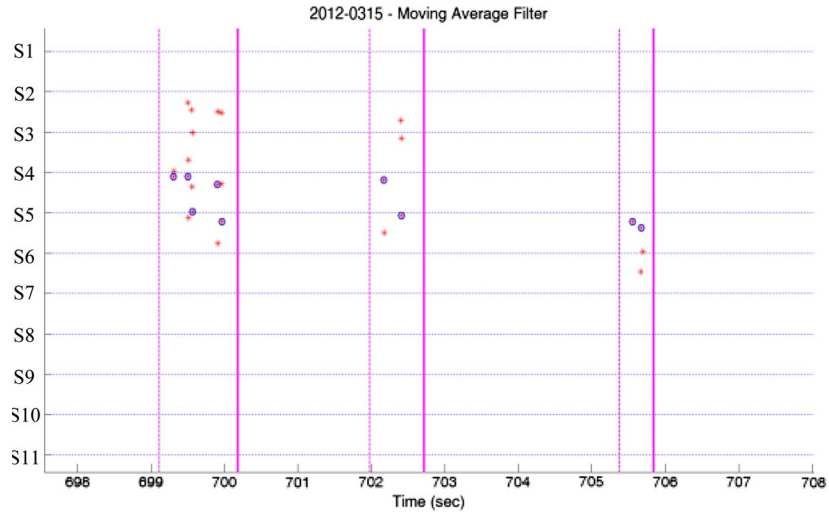

Fig. 8. Vehicle classification plot of the data set on March 15, 2012.

TABLE I
AVC PERFORMANCE WITH DIFFERENT SENSOR SETS

Scenario	Accelero-meter Sensor	Magneto-meter Sensor	2-axle Car	3-axle Car	5-axle Heavy Truck	Successful Classified	%
1	All	All	299	3	43	345	100%
2	L (8")	L & C	272	3	42	317	91.9%
3	R (6")	R & C	296	3	42	341	98.8%
4	All	C	285	3	38	326	94.5%
5	L (8")	All	277	3	43	323	93.6%
6	R (6")	All	298	3	43	344	99.7%
Video Image (ground truth)			299	3	43	345	–

2) Rush-Hour Validation: A 3.5-h data set from 5:20–8:50 A.M. was collected on April 18, 2012, to further evaluate the performance of the prototype AVC system in congested traffic conditions, as well as for a longer period. The 90-min rush hour (from around 7:20–8:50 A.M.) data are shown in Fig. 9, in which the colors of the vertical lines (peak clustering windows) indicate vehicle speed, as explained by the color bar, i.e., blue lines represent lower speed (i.e.,$<$ 30 mi/h), green and yellow lines represent medium speed (i.e., 30–50 mi/h), and red lines represent higher speed (i.e., $>$ 50 mi/h). The speed changes during the rush hour can be clearly seen. The lowest speed during the rush hour is 4.7 mi/h.

The total number of vehicles classified by the AVC system during the 90 min is 2253. However, it is very difficult to individually verify all the vehicles from the images. Considering the good performance from the previous image validation and the importance of classification of three-plus-axle vehicles, we randomly validate 5% of the major vehicle class at the study site (i.e., two-axle vehicles) and individually validate all the other three-plus-axle vehicles. All randomly selected 102 two-axle vehicles (Class 2–5) are correctly classified.

The performance for the 226 three-plus-axle vehicles is shown in Table II. The system successfully classified 223 vehicles in different classes, including a six-axle heavy truck,

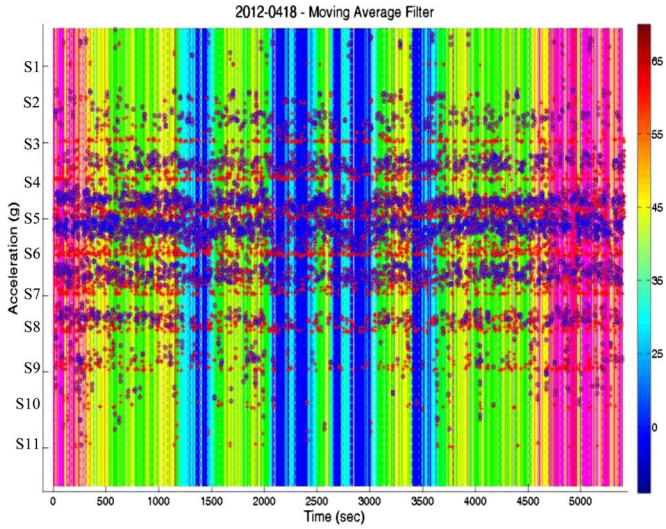

Fig. 9. 90-min rush-hour data on April 18, 2012.

TABLE II
IMAGE VALIDATION OF THREE-PLUS-AXLE VEHICLES UNDER RUSH HOUR

# of Axles	3	4	5	6	Total
Class	3/6/8	3/8	5/9/11	10	
AVC Output	15	7	203	1	226
Correct Classification	14	5	203	1	223

which has three tandem rear axles. Only three vehicles are not correctly classified during the 90-min rush hour, i.e., a semi-truck with a long-spacing trailer is classified as two vehicles, two bumper-to-bumper two-axle vehicles are classified as one four-axle vehicle at speed of 15.6 mi/h, and a five-axle heavy truck is classified as a four-axle vehicle because the peaks of two tandem axles are grouped into a single peak due to its low speed of 4.7 mi/h. Thus, the overall performance of the AVC system is very good under congested traffic conditions.

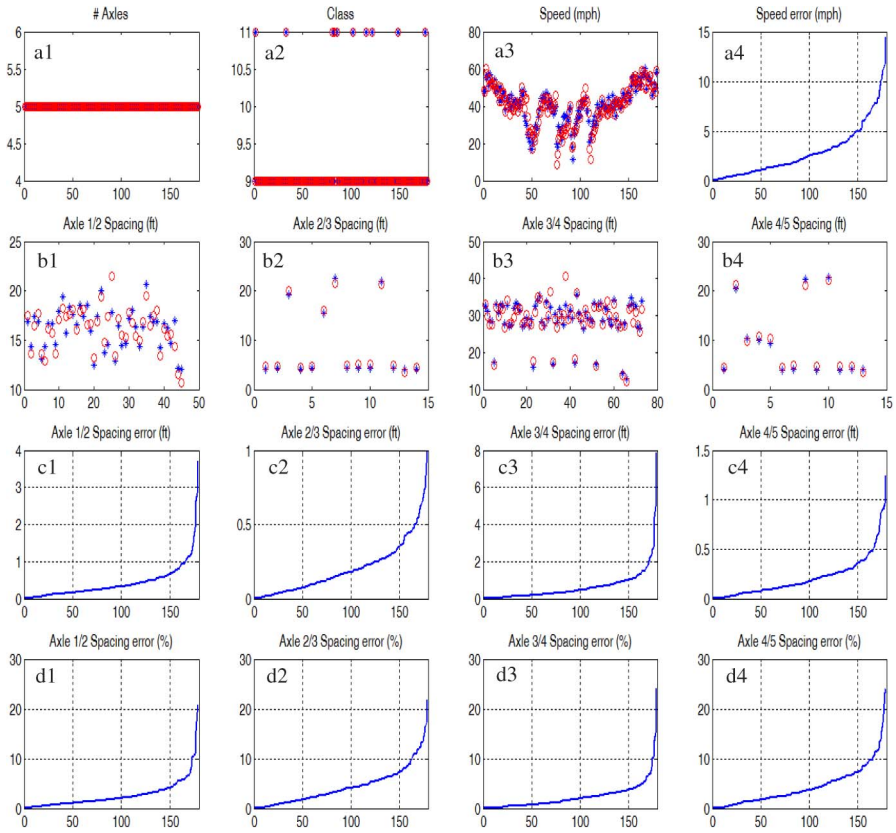

Fig. 10. Comparison of axle spacing of five-axle heavy trucks with WIM.

C. WIM Validation

Image validation is very accurate for vehicle count and classification. However, it is labor intensive and, thus, not suitable for a large data set. However, more importantly, video cannot be used to measure axle spacing. Therefore, reports from the nearby commercial WIM station are used as another ground truth to evaluate the performance of the prototype AVC system.

1) Axle Spacing: To evaluate the results of axle spacing, we first need to match vehicles detected by the two systems. Considering their sample size in the traffic stream and variation of the axle spacing of the vehicles, five-axle Class 9/11 heavy trucks are selected from the 90-min data set. One hundred seventy nine heavy trucks are matched, and the results are shown in Fig. 10. The blue stars are WIM data, and the red circles are AVC data. The horizontal axes are the number of samples. Fig. 10(a1) and (a2) shows the compared vehicles are those that we expected. The speed differences of all matched samples and their accumulated error are shown in Fig. 10(a3) and (a4). The matched samples with axle spacing differences larger than 0.5 ft are shown in sub-Fig. 10(b1)–(b4) (axle pairs 1/2, 2/3, 3/4, and 4/5, accordingly). The cumulative absolute axle spacing errors of all matched samples are shown in Fig. 10(c1)–(c4), and the cumulative percentage errors are shown in Fig. 10(d1)–(d4). The majority of the matched samples are Class 9 vehicles, which has two tandem axle pairs (2/3 and 4/5). As shown, the axle spacing calculated by the AVC system is very close to that from the commercial WIM station. The estimates of regular and tandem axle spacing are mostly within 1 and 0.5 ft, respectively, and 95% of the errors are within 5%. It should be noted that the errors are the composite of estimation errors in both the WIM and AVC systems.

TABLE III
HOURLY VEHICLE COUNTS COMPARING BETWEEN AVC AND WIM

April 18, 2012		Class 2–5 (2-axle)	Class 9 (5-axle)	Class 11 (5-axle)	All Classes (all-axles)
6 am – 7 am	AVC	1676	85	5	1785
	WIM	1679	86	6	1798
	diff	*3*	*1*	*1*	*13*
7 am – 8 am	AVC	1519	124	3	1661
	WIM	1523	124	4	1676
	diff	*4*	*0*	*1*	*15*

2) Vehicle Counts: The vehicle count report from WIM is used to validate the performance of the AVC system over a longer time. Two full hours' data (6:00–7:00 A.M. and 7:00–8:00 A.M.) are selected from the 3.5-h data set collected on April 18, 2012. The results are shown in Table III. Note that the classification scheme used by WIM is the Long-Term Pavement Performance (LTPP) [15], which uses not only axle spacing but also axle weights to classify vehicles. Vehicles in four categories, Classes 2–5, 9, 11, and all classes, are compared based on their definitions in both classification schemes. As shown, the vehicle counts for both hours matched very well. The small differences come from possible lane-changing vehicles, classification errors in both systems, time boundary effects, and definition differences between Scheme F and LTTP.

IV. Conclusion

This paper has described a reliable AVC prototype system using wireless sensors. The accelerometers are used to convert pavement vibration into axle locations, and the magnetometers are used to detect magnetic field changes and to estimate vehicle speed and peak clustering window. The sensor data are synchronized and processed in real time on the AP. Based on the calculated vehicle axle count and spacing, each vehicle is classified according to a predefined classification scheme, such as Scheme F.

A prototype AVC system was installed and tested on Interstate 80 at Pinole, CA, USA. Six sensor layout scenarios are evaluated in terms of accelerometer sensor spacing and sets of magnetometer sensors needed. System performance was evaluated using video images and reports from a nearby WIM station under both free and congested traffic. The video validation shows that the system classifies vehicles with accuracy of 99% for the recommended configuration, and the WIM validation shows that the system can generate a comparable report in terms of classification, axle spacing, and vehicle counts.

Future developments of this paper include the improvement of power efficiency to increase battery life. More field evaluations of the prototype AVC system are needed in different traffic environments, such as toll plazas and arterial corridors, where the traffic patterns are quite different.

Acknowledgment

The authors would like to thank Caltrans for allowing the installation of sensors on Interstate 80 and providing WIM reports, K. Kiani and G. Liu of Sensys Network Inc. for their help in assembling and testing the sensors, B. Wild for his earlier work in this study, and Dr. R. Kavaler for his supervision of the development of the sensor firmware.

References

[1] Y. Mimbela Luz Elena and L. A. Klein, *A Summary of Vehicle Detection and Surveillance Technologies Used in Intelligent Transportation Systems*. Washington, DC, USA: Fed. Highway Admin., Intell. Transp. Syst. Joint Program Off., 2000.

[2] S. Gupte and A. Papanikolopoulos, "Algorithms for vehicle classification," Minnesota Dept. Transp. (MnDOT), Saint Paul, MN, USA, Final Rep. MN/RC-2000-27, 2000.

[3] R. Martin, O. Masoud, S. Gupte, and A. Papanikolopoulos, "Algorithms for vehicle classification: Phase II," Minnesota Dept. Transp. (MnDOT), Saint Paul, MN, USA, Final Rep., MN/RC-2002-21, 2002.

[4] A. Y. Nooralahiyan, M. Dougherty, D. McKeown, and H. R. Kirkby, "A field trial of acoustic signature analysis for vehicle classification," *Transp. Res. Part C*, vol. 5, no. 3/4, pp. 165–177, Aug.–Oct. 1997.

[5] G. Zhang, Y. Wang, and H. Wei, "Artificial neural network method for length-based vehicle classification using single-loop outputs," *Transp. Res. Rec.*, vol. 1945, pp. 100–108, 2006.

[6] *Traffic Monitoring Guide*, Fed. Highway Admin., Washington, DC, USA, 2001.

[7] I. Urazghildiiev, R. Ragnarsson, P. Ridderstrom, A. Rydberg, E. Ojefors, K. Wallin, P. Enochsson, M. Ericson, and G. Lofqvist, "Vehicle classification based on the radar measurement of height profiles," *IEEE Trans. Intell. Transp. Syst.*, vol. 8, no. 2, pp. 245–253, Jun. 2007.

[8] B. Coifman and S. Kim, "Speed estimation and length based vehicle classification from freeway single loop detectors," *Transp. Res. Part C*, vol. 17, no. 4, pp. 349–364, 2009.

[9] A. Haoui, R. Kavaler, and P. Varaiya, "Wireless magnetic sensors for traffic surveillance," *Transp. Res. Part C*, vol. 16, no. 3, pp. 294–306, Jun. 2008.

[10] [Online]. Available: www.sensysnetworks.com

[11] S. Cheung and P. Varaiya, "Traffic surveillance by wireless sensor networks," California PATH Program Inst. Transp. Stud., Univ. California, Berkeley, CA, USA, Final Rep. UCB-ITS-PRR-2007-4, 2007.

[12] R. Bajwa, R. Rajagopal, P. Varaiya, and R. Kavaler, "In-pavement wireless sensor network for vehicle classification," in *Proc. IPSN*, 2011, pp. 85–96.

[13] J. H. Wyman, G. A. Braley, and R. I. Stevens, "Field evalualtion of FWHA vehicle classification categories, executive summary, materials and research," Fed. Highway Admin., Washington, DC, USA, Tech. Paper 84-5, 1985.

[14] R. Kavaler, K. Kwong, A. Raman, P. Varaiya, and D. Xing, "Arterial performance measurement system with wireless magnetic sensors," in *Proc. ICTIS*, 2011, pp. 377–385.

[15] Long Term Pavement Performance Program. [Online]. Available: http://www.fhwa.dot.gov/research/tfhrc/programs/infrastructure/pavements/ltpp/

Wenteng Ma (M'05) was born in China in 1976. He received the B.S. degree from Southeast University, Nanjing, China, in 1999; the M.E. degrees from the National University of Singapore, Singapore, and Pennsylvania State University, University Park, PA, USA, in 2002 and 2003, respectively; and the Ph.D. degree from the University of Minnesota, Minneapolis, MN, USA, in 2008, all in civil engineering.

From 2008 to 2011, he was a Principal Research Scientist with Citilabs, Alameda, CA, USA. Since 2011, he has been a Systems Engineer with Sensys Networks Inc., Berkeley, CA, USA. He has over ten years of professional experience in the fields of traffic engineering, transportation planning, intelligent transportation systems, wireless sensor networks, and software engineering.

Daniel Xing (M'06) received the B.S. and M.S. degrees in electrical engineering from the University of California, Los Angeles, CA, USA, in 2004 and 2005, respectively.

From 2006 to 2009, he was a Wireless Research Engineer with Toyota InfoTechnology Center, Mountain View, CA, USA. Since 2009, he has been with Sensys Networks Inc., Berkeley, CA, USA, working on various projects utilizing wireless sensor systems to capture speed, travel time, and classification. His research interests include wireless vehicular space, such as dedicated short-range communications and IEEE 802.11p.

Adam McKee received the B.S. degree in electrical engineering from the University of California, Davis, CA, USA, in 1993.

From 1994 to 1997, he was a Research Engineer with the DSP and Wireless Labs, Davis, CA, USA. Since 2008, he has been with Sensys Networks Inc., Berkeley, CA, USA, designing hardware platforms for processing and collecting data. He has 15 years of industry experience in the fields of data communications and telecommunications, which include GTE, Level One, Intel, McAfee, and Silicon Valley start-ups, implementing a wide variety of communication protocols. His research interests include the development and integration of various hardware platforms and interfaces.

Ravneet Bajwa received the B.Sc. and M.Sc. degrees from the University of California, Berkeley, CA, USA. He is currently working toward the Ph.D. degree in the Department of Electrical Engineering and Computer Science, University of California, Berkeley.

He is currently a Research Scientist with Sensys Networks Inc., Berkeley, working on the use of wireless accelerometers for automatic vehicle classification and weighing in motion.

Christopher Flores (M'78–SM'84) received the B.Tech. degree in electrical engineering from the Indian Institute of Technology, Kanpur, India, in 1978 and the M.S. and Ph.D. degrees from the University of California, Berkeley, CA, USA, in 1981 and 1983, respectively.

He started his career with Bell Laboratories and spent 25 years in telecommunications, including engineering design and management positions, at a number of start-ups developing wireless systems for cellular and local loop applications. He switched to transportation in 2010 with the goal of bringing wireless-based innovations to the challenges in the transportation sector. He is currently a Director of Advanced Technology with Sensys Networks Inc., Berkeley.

Brian Fuller received the B.Sc. degree in electrical engineering from Pennsylvania State University, University Park, PA, USA, in 1990.

He has over 16 years of product design and development experience in data networking and telephony. He was a Director of Hardware Engineering with GoDigital Networks, managing the extensive growth of the company's digital subscriber line technologies while designing patented systems for their broadband access products. He has held both technical and managerial responsibilities with Odyssia Systems (now Extreme Networks, Inc.), Diva Communications (now InnoMedia, Inc.), and OcTel Communications (now Lucent Technologies, Inc.). He is currently the Vice President of Engineering with Sensys Networks Inc., Berkeley, CA, USA.

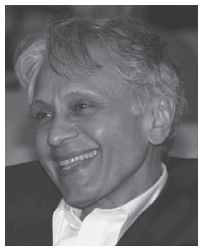

Pravin Varaiya (M'68–SM'78–F'80) received the Ph.D. degree in electrical engineering and computer sciences from the University of California, Berkeley, CA, USA in 1966.

From 1975 to 1992, he was a Professor of economics with the University of California, Berkeley. He is currently a Professor with the Graduate School, Department of Electrical Engineering and Computer Sciences, University of California, Berkeley. He is a Cofounder of the Sensys Networks, Inc. His current research interests include transportation networks and electric power systems.

Prof. Varaiya is a member of the National Academy of Engineering and a Fellow of the American Academy of Arts and Science. He received a Guggenheim Fellowship, three Honorary Doctorates, the Field Medal and the Bode Prize of the IEEE Control Systems Society, the Richard E. Bellman Control Heritage Award, and the Outstanding Research Award of the IEEE Intelligent Transportation Systems Society.